

Chapter 33

Cooper pair correlations and energetic knock-out reactions

E. C. Simpson and J. A. Tostevin

*Department of Physics, Faculty of Engineering and Physical Sciences,
University of Surrey, Guildford, Surrey GU2 7XH, United Kingdom*

Two-nucleon removal (or knock-out) reactions at intermediate energies are a developing tool for both nuclear spectroscopy and for the study of certain nucleon correlations in very exotic and some stable nuclei. We present an overview of these reactions with specific emphasis on the nature of the two-nucleon correlations that can be probed. We outline future possibilities and tests needed to fully establish these sensitivities.

1. Fast two-nucleon removal reactions

The ability to probe experimentally the spin-structure of nuclear wave functions and, in particular, to identify and quantify spin-singlet, $S=0$, nucleon-pair components is a long-standing ambition. Low-energy two-nucleon transfer studies between light-ions, such as the (p,t) reaction, studied extensively as such a probe for stable nuclei and, more recently, for exotic nuclei, are discussed in several Chapters in this volume.¹ In such reactions the light-ion transfer vertex, here $\langle p | t \rangle$, selects, predominantly, $S=0$ two-neutron pairs (specifically, 1s_0 , $T=1$ configurations) from the projectile ground-state wave function; as is most transparent under the assumption that the reaction proceeds as a direct one-step pair transfer.

Intermediate-energy two-nucleon removal reactions offer a relatively new and developing experimental approach. The reactions have developed out of the need for efficient detection and use of a more restricted set of observables in experiments with rare isotope beams. The usually highly-unstable projectile nuclei of mass $A+2$ are produced as fast, low-intensity secondary beams by fragmentation and fragment separation. The beams, typically with incident energies of >80 MeV per nucleon and $v/c \geq 0.35$, collide with light target nuclei, e.g. beryllium or carbon. Our interest here is in collision

events that remove two nucleons (2N) with and without inelastic excitation of the target nucleus. These 2N removal events populate the (bound or unbound) ground and excited states of the mass A projectile-like residual nuclei. Measurements of the yields and final momenta of these forward-travelling residues also probe aspects of the structure and 2N correlations in the projectile wave function. This Chapter discusses this dependence of 2N-removal reaction observables on the structure and also the spin S of the 2N pair. The observables discussed are inclusive with respect to the fate and final states of the target and of the removed nucleons. We comment briefly later on the potential of future data, when more exclusive measurements of these reaction fragments become practical.

The present developments have evolved from first investigations whose focus was one-neutron removal from halo nuclei.² Narrow parallel (beam-direction) residue momentum distributions were observed,^{3,4} characteristic of the last weakly-bound neutron occupying single-particle states of low orbital angular momentum ℓ . More generally, these momentum distribution widths increase with both ℓ and the separation energy of the removed nucleon³ permitting an assessment of structure model predictions of e.g. level orderings and single-nucleon spectroscopic strengths⁵⁻⁷ from measured final-state exclusive yields and the residue momenta.

Our focus is on 2N removal reactions for structure studies of exotic nuclei.⁸⁻¹⁴ The theoretical description of the reaction, developed to incorporate correlated shell-model 2N overlap functions,^{15,16} has been used to formulate the momentum distributions of these reaction residues^{17,18} and their sensitivity¹⁹ to nuclear structure. We will discuss how, although the removal reaction mechanism makes no intrinsic selection of the spin S of nucleon pairs at the projectile surface, the 2N removal events are highly selective geometrically, probing the 2N joint-position-probability $\rho_f(\mathbf{r}_1, \mathbf{r}_2)$ appropriate to a given final state f . It follows that pair removal is enhanced when nucleons have a spatial (proximity) correlation in the projectile ground-state. The dimensions of the probed volume are of the same size (2-3 fm) as has been predicted²⁰ for Cooper pairs at the nuclear surface.

2. Two-nucleon removal: structure input

We review the salient points of the two-nucleon removal reaction formalism, developed in Refs. 15-19, to make clear the connection between structure, residue yields, and their momentum distributions. We assume transitions from the projectile initial state i , with spin (J_i, M_i) , to particular residue

final states f , and (J_f, M_f) . The residues are assumed to be spectators in the sudden reaction description¹⁵ and the states f are not coupled to the reaction dynamics. The structure input to the reaction is determined by the projectile and residue 2N overlaps

$$\Psi_i^{fM_f}(1, 2) = \sum_{I\mu T\alpha} (I\mu J_f M_f | J_i M_i) (T\tau T_f \tau_f | T_i \tau_i) C_\alpha^{IT} [\overline{\psi_{\beta_1} \otimes \psi_{\beta_2}}]_{I\mu}^{T\tau},$$

where α runs over the set of contributing spherical configurations (β_1, β_2) of the two-nucleons, with $\beta \equiv (n\ell j)$. The C_α^{IT} are the two-nucleon amplitudes (TNA) for each configuration for total angular momentum I and isospin T of the two nucleons and a given $i \rightarrow f$ transition. The square bracketed term is the antisymmetrized 2N wave function written in jj -coupling. Truncated-basis shell-model calculations have, thus far, provided the structure input, via the TNA, giving good agreement with measured final state branching ratios¹⁶ for nuclei in the sd -shell.

In the following we identify in some detail the role of the 2N spin S in the calculations and the observables. Thus we reexpress the overlap and subsequent derived properties in LS -coupling.¹⁹ The coherence or otherwise of the reaction observables to the different LS terms in the overlaps is clarified through the associated 2N joint position probabilities $\rho_f(\mathbf{r}_1, \mathbf{r}_2)$.

When assuming eikonal reaction dynamics the probabilities for absorption (a , an inelastic event) or transmission (e , an elastic event) of a fragment p (the nucleons or the residue) in a collision with the target are $P_a(b_p) = [1 - |S_p(b_p)|^2]$ and $P_e(b_p) = [1 - P_a(b_p)] = |S_p(b_p)|^2$, where $S_p(b_p)$ is the fragment-target elastic S-matrix at its impact parameter b_p . These factors, due to the effects of strong absorption in the S_p , have the property that $P_a(b_p) \rightarrow 1$ and $P_e(b_p) \rightarrow 0$ at small impact parameters. This leads to a natural surface localization of the 2N removal reaction events where the mass A residue is transmitted and two nucleons are found sufficiently close together that both interact strongly with the light (small) target nucleus and are removed from the projectile.

Furthermore, if the $P_{a,e}$ factors are spin-independent, as is assumed here, then the 2N removal cross section and its differential with respect to the residue momenta involve only the squared modulus of the 2N overlap summed over the two nucleons, residue and projectile spin projections¹⁷

$$\rho_f(\mathbf{r}_1, \mathbf{r}_2) = \frac{1}{j_i^2} \sum_{M_i M_f} \langle \Psi_i^{fM_f} | \Psi_i^{fM_f} \rangle_{sp}. \quad (1)$$

So, a transition to a given final state f will probe the details of this ρ_f ,

specifically, the degree of 2N spatial correlations at the projectile surface. This joint-probability is incoherent with respect to contributions from different I , L and S . Its dependence on the 2N correlations is best presented in terms of radial and angular correlation functions. Explicitly,

$$\rho_f(\mathbf{r}_1, \mathbf{r}_2) = \sum_{LSI} \left\{ \sum_{\alpha\alpha'} \mathfrak{C}_{\alpha LS}^{IT} \mathfrak{C}_{\alpha' LS}^{IT} D_\alpha D_{\alpha'} \right. \\ \left. \times [U_{\alpha\alpha'}^D(1, 2) \bar{\Gamma}^{L,D}(\omega) - (-)^{S+T} U_{\alpha\alpha'}^E(1, 2) \bar{\Gamma}^{L,E}(\omega)] \right\}$$

with $D_\alpha = 1/\sqrt{2(1 + \delta_{\beta_1\beta_2})}$. The $\mathfrak{C}_{\alpha LS}^{IT}$ are the LS -coupled TNA

$$\mathfrak{C}_{\alpha LS}^{IT} = \hat{j}_1 \hat{j}_2 \hat{L} \hat{S} \left\{ \begin{array}{ccc} \ell_1 & s & j_1 \\ \ell_2 & s & j_2 \\ L & S & I \end{array} \right\} C_\alpha^{IT}. \quad (2)$$

Here $U_{\alpha\alpha'}^D$ describes the radial correlation of the active single-particle states,

$$U_{\alpha\alpha'}^D(1, 2) = u_{\beta_1}(1)u_{\beta_2}(2)u_{\beta_1'}(1)u_{\beta_2'}(2) + u_{\beta_2}(1)u_{\beta_1}(2)u_{\beta_2'}(1)u_{\beta_1'}(2),$$

and $\beta_1' \leftrightarrow \beta_2'$ in the analogous exchange term U^E . The 2N angular correlations, $\bar{\Gamma}^L$, are independent of S and are determined only by the active orbital set $\{\alpha \equiv (\beta_1, \beta_2)\}$ and L . This angular correlation function is^{19,21}

$$\bar{\Gamma}^{L,D}(\omega) \equiv \bar{\Gamma}_{\ell_1\ell_2\ell_1'\ell_2'}^{L,D}(\omega) = (-1)^L \frac{\hat{\ell}_1 \hat{\ell}_1' \hat{\ell}_2 \hat{\ell}_2'}{(4\pi)^2} \sum_k W(\ell_1\ell_2\ell_1'\ell_2'; Lk) \\ \times (-1)^k (\ell_1 0 \ell_1' 0 | k 0) (\ell_2 0 \ell_2' 0 | k 0) P_k(\cos \omega), \quad (3)$$

where $\cos \omega = \hat{\mathbf{r}}_1 \cdot \hat{\mathbf{r}}_2$ is the 2N angular separation. The exchange term is

$$\bar{\Gamma}^{L,E}(\omega) = (-)^{\ell_1 + \ell_2 - L} \bar{\Gamma}_{\ell_1\ell_2\ell_2'\ell_1'}^{L,D}(\omega).$$

Here we do not show the (now implicit) sum on isospin T and the squared isospin coefficient $(T\tau T_f \tau_f | T_i \tau_i)^2$ which are defined trivially in each case. It is also important to note that an $[S, T]=[0, 1]$ contribution in the above does not imply a 1s_0 two-nucleon pair, although this is expected to be the dominant configuration with these quantum numbers.

3. Sensitivity of observables to structure

This formal discussion has defined the $S=0$ 2N components present in the projectile wave function that will be delivered to the target nucleus. As noted, the primary elastic and inelastic removal probabilities offer no direct selection on the S of the removed nucleons. The target intercepts the

2N density ρ_f near the projectile surface and $S=0$ pairs will be removed with all other LSI terms; all terms making additive contributions to the cross sections. The relative strengths of the $S=0, 1$ components are therefore entirely determined by the nuclear structure. Since the sums over the contributing configurations α are coherent, both the sizes and phases of the TNA are key factors. The $S=0, 1$ relative strengths of each α is determined by the $9j$ -coefficient in Eq. 2. Since, most often, the (exotic) projectiles have spin $J_i=0$, I is fixed and equal to the final state spin J_f .

3.1. Spin selection and L -sensitivity

Critically, the S are coupled to the 2N total orbital angular momentum values L . Each L contributes a cross section momentum distribution with a characteristic width.^{17,18} In general these widths show a robust increase with L (and hence I), and a weaker, transition-dependent sensitivity to the contributing 2N configurations α . Most simply, ground-state to ground-state 2N removal from even-even nuclei, with $I=0$ and hence $S=L=0$ or $S=L=1$, may highlight significant deviations and test structure model predictions. The differences in momentum widths for $L=0$ and $L=1$ are however relatively modest so high statistics measurements are necessary. For excited final-states the momentum distributions will be characteristic of the LS content of ρ_f . In many cases¹⁹ final-states of the same J_f will have a sufficiently different LS make-up to affect their residue momentum distributions. So, interpretation of observables is not trivial and the calculated cross sections are now more intimately (and opaquely) connected to the nuclear structure; here the TNA. In particular, the $S=0$ pair sensitivity of the reaction is not a generic feature and must be considered on a case-by-case basis. In the sd -shell example used below, for $^{28}\text{Mg}(-2p)$, the S content of ρ_f is seen to vary markedly with the final state J_f , a result of the interplay of the structure and $9j$ -couplings in Eq. 2. Coincidence final-state measurements that are exclusive with respect to the residue final states are thus vital. More exclusive measurements, for example if one can observe correlations of the removed nucleons in the final states, may offer additional probes of these projectile (entrance channel) spin correlations.

Applications of 2N knockout have, to date, concentrated on nuclei with $A < 60$, the shell-model providing the input to compute the ρ_f . Typically, the shell-model predicts appreciable strength to relatively simple 2N-hole states. For even-even sd -shell nuclei the $J_f=0^+$ ground-states are strongly populated, with significant yields also to low-lying 2^+ and 4^+ states. We

illustrate this situation with reference to 2p-removal from neutron-rich ^{28}Mg projectiles at 82 MeV per nucleon incident energy. In other cases¹⁴ there can be significant changes in the nuclear structures between the projectile and residue states leading to a greater fragmentation of the TNA strengths and a more complex interpretation of the cross sections.

In the sudden plus eikonal approximations used, the projectile travels and grazes the target moving in the z (the beam) direction. So, it is intuitive to construct the projection of $\rho_f(\mathbf{r}_1, \mathbf{r}_2)$ onto the plane perpendicular to the beam direction by integration over the z_i of the two nucleon positions $\mathbf{r}_i=(\mathbf{s}_i, z_i)$. This maps out the pair position probability distribution (including with respect to S) to that seen by the target nucleus. We denote these projected densities $\mathcal{P}_{J_f}(\mathbf{s}_1, \mathbf{s}_2)$. As was detailed above, the spatial correlations of the two nucleons are concisely expressed as a function of their angular separation, ω . Clearly the z_i -integrated joint probabilities \mathcal{P}_{J_f} are a convoluted form of this correlation function, each fixed $(\mathbf{s}_1, \mathbf{s}_2)$ sampling a range of ω . However, since the reaction is surface localized and the target is light (small) the effective z_i thicknesses are small and the \mathcal{P}_{J_f} continue to make a valuable intuitive link between the 2N spatial (and spin and orbital angular momentum) correlations and their removal cross sections.

3.2. *sd-shell example: $^{28}\text{Mg}(-2p)$*

Figures 1 and 2 show calculations of the impact parameter plane two-nucleon probabilities \mathcal{P}_{J_f} seen by the target nucleus, computed from the USD shell-model TNA¹⁵ and overlaps, for the $^{28}\text{Mg} \rightarrow ^{26}\text{Ne}(J_f^\pi)$ 2p removal transitions. The left panels show the \mathcal{P}_{J_f} for all spin $S(=0,1)$ components. The right panel of Fig. 1 shows the corresponding \mathcal{P}_{J_f} assuming that removal is from a pure $\pi[1d_{5/2}]^2$ configuration. The right panel of Fig. 2 shows $\mathcal{P}_{J_f}^{S=0}$ computed using only the $S=0$ wave function components. The $S=0$ component in the case of the ground-state to ground-state transition of Fig. 1 (left) is essentially indistinguishable and is not shown. Figure 1 shows the additional spatial correlations introduced by configuration mixing in the full *sd*-shell-model calculation. A known feature¹⁹ of the ρ_f is their symmetry about $\omega=\pi/2$ if all of the active nucleon orbitals β_i are in the same major shell (here the *sd*-shell); specifically, if they have the same parity. In the \mathcal{P}_{J_f} contour plots shown below, this is a symmetry about the y -axis if one of the nucleons, say \mathbf{s}_1 , is found at the surface on the x -axis (indicated by a back spot). The figures, drawn with the same position probability scales, are for the 0^+ transition, Fig. 1, and for the sum of overlaps

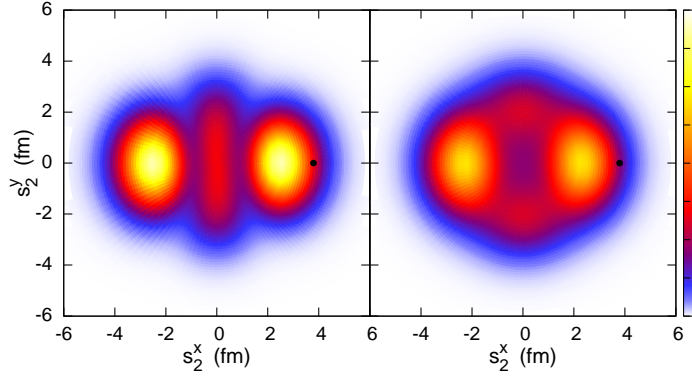


Fig. 1. Calculated $\mathcal{P}_{J_f=0}(s_1, s_2)$ for 2p removal to the $^{26}\text{Ne}(0^+)$ ground-state. Nucleon 1 is at the position of the black spot on the x -axis. The left panel uses the full sd -shell TNA. The right panel assumes a pure $\pi[1d_{5/2}]^2$ configuration.

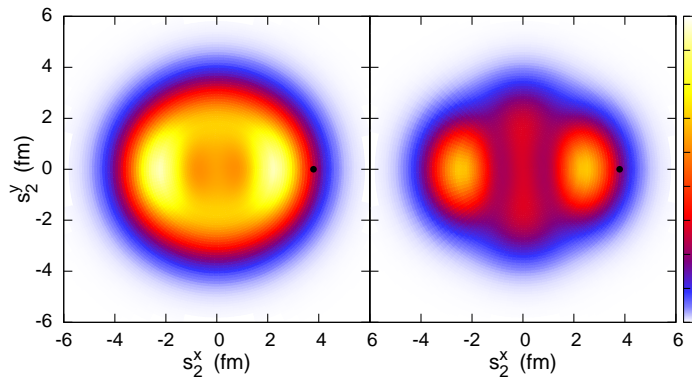


Fig. 2. Calculated $\mathcal{P}_{\text{incl}}(s_1, s_2)$ for inclusive 2p removal to the $^{26}\text{Ne}(0^+, 2_1^+, 4^+, 2_2^+)$ final states. The left panel includes all LS components. The right panel shows $\mathcal{P}_{\text{incl}}^{S=0}(s_1, s_2)$ and includes only the $S=0$ components of the overlaps.

for the 0^+ , 2_1^+ , 4^+ and 2_2^+ transitions, Fig. 2; the latter are relevant to the inclusive cross section. The dominance of the $S=0$ component in the 0^+ ground state transition and the importance of both the 0^+ transition and of $S=0$ 2p pairs to the inclusive cross section are evident.

To further illustrate the reaction mechanism's relative transparency to the S of the nucleon pairs delivered by the projectile, in Table 1 we show the computed partial and the inclusive cross sections for these \mathcal{P}_{J_f} . The $S=0$ fractions(%) of the overlaps and the cross sections show a small, state-dependent enhancement of $S=0$ terms in the cross sections, but that the

Table 1. Calculated and experimental partial and inclusive cross sections for $^{28}\text{Mg}(-2\text{p})$ at 82 MeV per nucleon, see also Ref. 15. The percentage contributions of $S=0$ terms to the overlaps and the cross sections are also shown.

J_f^π	E^* (MeV)	$\rho_f(S=0)$ (%)	σ_{exp} (mb)	σ_{th} (mb)	$\sigma_{S=0}$ (mb)	$\sigma_{S=0}$ (%)
0^+	0.0	86	0.70(15)	1.190	1.083	90
2^+	2.02	18	0.09(15)	0.327	0.071	22
4^+	3.50	38	0.58(9)	1.046	0.523	49
2_2^+	3.70	50	0.15(9)	0.458	0.250	54
Inclusive			1.50(10)	3.02	1.93	64

spin content of the projectile wave-function is reflected in the calculated cross sections. Here the $S=0$ terms are seen to be responsible for 64% of the computed inclusive cross section.

3.3. Cross shell excitations

It is known^{22–26} that the presence of 2N configurations α with β_1 and β_2 of opposite parity, e.g. via $n\hbar\omega$, $n = \text{odd}$, single-particle excitations, generate surface pairing. In Eq. 3 such configurations remove the angular symmetry about $\omega = \pi/2$ by introducing odd K Legendre terms. Whether these odd-even combinations are constructive (destructive) in (de)localizing pairs will depend, case-by-case, on the TNA, the signs of the $9j$ -coefficients, and the $\bar{\Gamma}^L(\omega)$ for $\omega \approx 0$. The 2N removal mechanism is clearly sensitive to such coherent cross-shell admixtures. Such sensitivity is illustrated in Fig. 3 for the $^{48}\text{Ca}(-2\text{n})$ ground-state to ground-state overlap. Here the cross-shell admixtures, over several oscillator shells, were estimated perturbatively (see Eq. 2 of Ref. 22) from realistic, N3LO V_{lowk} , two-body matrix elements²⁷ from an assumed $\nu[1f_{7/2}]^2$ configuration. The cross-shell admixtures are seen to enhance the 2n spatial correlations and the 2N removal cross section.

There are significant experimental challenges to measurements for such a neutron-rich 2n removal case. The valence neutrons of ^{48}Ca are less bound than the protons and ^{46}Ca will also be produced by population and neutron-decay of neutron-unbound states in ^{47}Ca . The means to distinguish such direct and indirect paths, by fast-neutron detection, are however advanced. The influence of such cross-shell excitations on 2N removal should be quantified for nuclei at or near closed shells. The $^{16}\text{O}(-2\text{n})$ reaction, where only the ^{14}O residue ground state is bound, would provide a valuable test case.

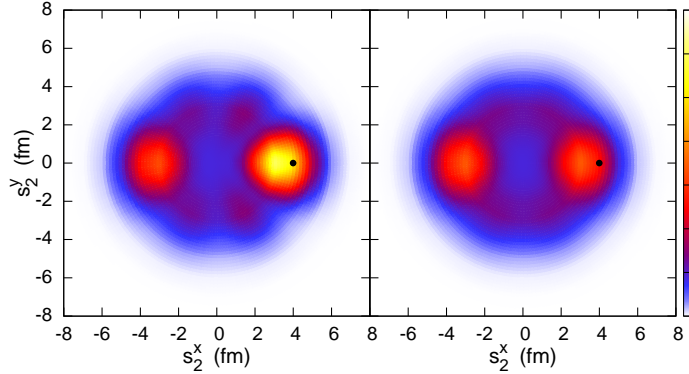


Fig. 3. Ground-state to ground-state $\mathcal{P}_{J_f=0}(s_1, s_2)$ for the $^{48}\text{Ca}(-2n)$ overlap. Nucleon 1 is at the position of the black spot on the x -axis. The left panel uses the multi-shell TNA set (see the text). The right panel is for removal of a pure $\nu[1f_{7/2}]^2$ pair.

4. Experimental considerations and future outlook

A major thrust of experimental activity is toward increasingly exotic nuclides whose low-lying spectra are unknown and are often in the continuum. The importance of nucleon removal reactions derives from their detection efficiency (near 100%) and use of thick reaction targets, increasing the effective luminosity of the low intensity exotic beams. Since, as presently measured, the experimental 2N cross sections are inclusive with respect to the final states of the target and the removed nucleons, they are relatively large. Nevertheless, accessible observables remain constrained by low beam intensity to: (a) the decay γ -rays of the reaction residues, that allow extraction of (b) final-state-exclusive residue cross sections, and (c) the differential of these cross sections with respect to the residue parallel momenta. The importance of the shapes and widths of these momentum distributions as a probe of L (and S) has been stressed. A barrier to sufficiently precise momentum measurements is the broadening of the residue momenta (in charge changing reactions) due to the unknown reaction point in the thick target. This problem can be mitigated, when needed, by the use of thin targets, but at the cost of reduced yields.

The discussions here focus on the structure sensitivity of the direct 2N removal mechanism. The examples used are for two like nucleons ($T=1$). These theoretical sensitivities are valid for 2n, 2p or np-pair removal, independent of the energies of the Fermi surfaces of the nucleon species. These direct cross sections can and have been measured rather cleanly, enabled

by the relevant separation energy thresholds,^{8,15} when the two nucleons are initially strongly-bound in the projectile. Thus 2p (2n) removal from neutron-rich (deficient) systems are the most accessible. The removal of weakly bound nucleons (and np pairs) is in general more complicated. The mass A residues can often be populated strongly by indirect paths, involving single-nucleon removal to and subsequent decay of intermediate, mass $A+1$ particle-unbound states. Without an effective experimental discrimination between direct and indirect events, 2N removal reactions cannot yet be applied to study correlations of e.g. weakly-bound 2n pairs in near-dripline neutron-rich nuclei.²⁸ Light $N=Z$ nuclei are an exception.²⁹ They permit further detailed tests of the reaction sensitivities for both $T=0$ and $T=1$ 2N pairs in systems where proton-neutron pairing is significant. New high-statistics measurements for such systems, where there is far less ambiguity in the underlying nuclear structure, are possible and necessary.

Truncated-basis shell-model calculations have provided the structure touchstone for the prototype 2N removal studies to date, but the description of the reaction dynamics is indifferent to the structure model. The connection to alternative structure model predictions is most simply made through the computed $\rho_f(\mathbf{r}_1, \mathbf{r}_2)$. Coupling of the existing eikonal reaction dynamics to alternative structure models will provide the means to study quantitatively those regions of rapidly changing structure associated with the onset of deformation,^{10,12-14} and heavier mid-shell nuclei in transitional regions. One- and two-nucleon spectroscopic amplitudes using BCS wave functions, written³⁰⁻³² in terms of the occupation amplitudes, v_k and u_k , have been widely used in transfer reaction studies.³³⁻³⁵ These amplitudes are eminently applicable and necessary for future studies of heavier nuclei. As was also discussed, 2N removal observables will be sensitive to the mixing of opposite parity orbitals in the 2N overlap function. The degree of mixing will depend strongly on the chosen set of single-particle energies, perhaps influenced by deformation of the projectile, and by the strength of the pairing interaction. Quantification of these sensitivities offers exciting future prospects and challenges to theory and experiment.

We have illustrated the 2N removal reaction mechanism for lighter nuclei where prototype data sets are available for beams with modest intensity. The available data remain limited in scope and in statistical precision. An important development in these lighter systems will be to also detect the removed nucleons in the final-state and, if possible, to quantify the degree to which they are correlated. The possibility to connect any such final-state 2N correlations to those delivered by the projectile in the entrance

channel, as were discussed here, will be of considerable interest. Studies in heavier projectiles will bring practical complications. A first study of the $^{208}\text{Pb}(-2\text{p})$ reaction,³⁶ with many available valence protons and a significantly higher residue level density, predict significant populations of 52 final states below the ^{206}Hg separation energy. Such final-state complexity presents major challenges.

5. Summary

We have discussed the 2N correlations in a projectile wave function that can be probed, in principle, using the fast, direct 2N removal reaction mechanism. We have shown that the geometric selectivity of the reaction on light target nuclei favours configurations, and coherent sums thereof, that result in a high degree of spatial localization of pairs of nucleons near the projectile surface. Access to specific information on the spin components of the wave function is possible due to their LS -coupling and the dependence of the widths of residue momentum distributions to these L components. High-statistics measurements of partial cross sections to the residue final states, of their momentum distributions, and of more exclusive observables will be needed to fully and quantitatively test these sensitivities.

Acknowledgements

This work was supported by the United Kingdom Science and Technology Facilities Council (STFC) under Grants ST/F012012 and ST/J000051.

References

1. Chapters 26 Kanungo and Tanihata, 27 Navin, 28 Von Oertzen, 31 Hansen, 32 Thompson and Brown, and 34 Potel and Broglia, of this Volume.
2. N. A. Orr *et al.*, *Phys. Rev. Lett.* **69**, 2050 (1992); *Phys. Rev. C* **51**, 3116 (1995).
3. P. G. Hansen, *Phys. Rev. Lett.* **77**, 1016 (1996).
4. P. G. Hansen, J. A. Tostevin, *Ann. Rev. Nucl. Part. Sci.* **53**, 219 (2003).
5. B. A. Brown, P. G. Hansen, B. M. Sherrill, J. A. Tostevin, *Phys. Rev. C* **65**, 061601(R) (2002).
6. A. Gade *et al.*, *Phys. Rev. Lett.* **93**, 042501 (2004).
7. A. Gade *et al.*, *Phys. Rev. C* **77**, 044306 (2008).
8. D. Bazin *et al.*, *Phys. Rev. Lett.* **91**, 012501 (2003).
9. K. Yoneda *et al.*, *Phys. Lett.* **B499**, 233 (2001); *Phys. Rev. C* **74**, 021303 (2006).

10. A. Gade *et al.*, *Phys. Rev. Lett.* **99**, 072502 (2007); *Phys. Rev. C* **76**, 024317 (2007).
11. B. Bastin *et al.*, *Phys. Rev. Lett.* **99**, 022503 (2007).
12. P. Adrich *et al.*, *Phys. Rev. C* **77**, 054306 (2008).
13. P. Fallon *et al.*, *Phys. Rev. C* **81**, 041302(R) (2010).
14. D. Santiago-Gonzalez *et al.*, *Phys. Rev. C* **83**, 061305(R) (2011).
15. J. A. Tostevin, G. Podolyák, B. A. Brown, P. G. Hansen, *Phys. Rev. C* **70**, 064602 (2004).
16. J. A. Tostevin, B. A. Brown, *Phys. Rev. C* **74**, 064604 (2006).
17. E. C. Simpson, J. A. Tostevin, D. Bazin, B. A. Brown, A. Gade, *Phys. Rev. Lett.* **102**, 132502 (2009).
18. E. C. Simpson, J. A. Tostevin, D. Bazin, A. Gade, *Phys. Rev. C* **79**, 064621 (2009).
19. E. C. Simpson, J. A. Tostevin, *Phys. Rev. C* **82**, 044616 (2010).
20. M. Matsuo, K. Mizuyama, Y. Serizawa, *Phys. Rev. C* **71**, 064326 (2005); N. Pillet, N. Sandulescu, P. Schuck, *Phys. Rev. C* **76**, 024310 (2007).
21. G. F. Bertsch, R.A. Broglia, C. Riedel, *Nucl. Phys.* **A91**, 123 (1967).
22. W. T. Pinkston, *Phys. Rev. C* **29**, 1123 (1984).
23. F. A. Janouch, R. J. Liotta, *Phys. Rev. C* **27**, 896 (1983).
24. F. Catara, A. Insolia, E. Maglione, A. Vitturi, *Phys. Rev. C* **29**, 1091 (1984); *Phys. Lett.* **B149**, 41 (1984).
25. A. Insolia, R. J. Liotta, E. Maglione, *J. Phys. G* **15**, 1249 (1989).
26. M. A. Tischler, A. Tonina, G. G. Dussel, *Phys. Rev. C* **58**, 2591 (1998).
27. B. A. Brown, private communication (2010).
28. E. C. Simpson, J. A. Tostevin, *Phys. Rev. C* **79**, 024616 (2009).
29. E. C. Simpson, J. A. Tostevin, *Phys. Rev. C* **83**, 014605 (2011).
30. S. Yoshida, *Phys. Rev.* **123**, 2122 (1961); *Nucl. Phys.* **33**, 685 (1962).
31. R. A. Broglia, C. Riedel, T. Udagawa, *Nucl. Phys.* **A135**, 561 (1969).
32. R. J. Ascutto, N. K. Glendenning, *Phys. Rev. C* **2**, 415 (1970).
33. J. Kern, O. Mikoshiba, R. K. Sheline, T. Udagawa, S. Yoshida, *Nucl. Phys.* **A104**, 642 (1967).
34. T. Takemasa, M. Sakagami, M. Sano, *Phys. Lett.* **B37**, 473 (1971); *Phys. Rev. Lett.* **29**, 133 (1972).
35. M. Guttormsen, T. Pedersen, J. Rekstad, T. Engeland, E. Osnes, F. Ingelbretsen, *Nucl. Phys.* **A338**, 141 (1980).
36. E. C. Simpson, J. A. Tostevin, Zs. Podolyák, P. H. Regan, S. J. Steer, *Phys. Rev. C* **80**, 064608 (2009); **82**, 037602 (2010)